

ANSYS[®]**Alcon**[®]

MODELLING OCULAR DELIVERY USING COMPUTATIONAL FLUID DYNAMICS

In this piece, Paul Missel, PhD, Therapeutic Area Modeller, Modelling & Simulation, Global Clinical and Regulatory Affairs, Alcon Research Ltd, and Marc Horner, PhD, Lead Technical Services Engineer, Healthcare, ANSYS, Inc, describe the use of computational fluid dynamics simulations to predict drug flow and temperature inside the eye, and provide examples of applications modelling: delivery following topical application; delivery from an intra-ocular depot; and delivery from juxtascular devices.

INTRODUCTION

Effective drug delivery to internal ocular tissues must overcome significant barriers imposed by fluid flow and clearance within the eye. Fluid flow processes include production, circulation and elimination of both tear fluid and aqueous humour, and hydraulic-assisted flow through porous media such as the vitreous humour, iris root, and outer sheath tissues. Clearance occurs as dissolved drug flows past or percolates through vascular tissues such as the conjunctiva, iris, ciliary body, retina and choroid or into the lymphatic system. Computer modelling is helping pharmaceutical scientists understand the interplay between drug formulation, fluid flow and clearance, which is leading to the development of more effective ocular drug delivery systems.

Classical pharmacokinetic (PK) models were among the first models developed for predicting ocular drug disposition. These models are comprised of well-mixed compartments representing specific ocular tissues with various interconnections. A series of first-order transfer equations describes transport between and elimination from each compartment. Physiologically-based pharmacokinetic (PBPK) approaches improve on PK models by incorporating the flow processes that facilitate drug distribution within the eye and drug clearance through vascular tissues. This is accomplished by constructing model compartments explicitly reflecting the volumes of the tissues they represent, by replicating the physiological production and elimination of tear fluid and aqueous humour and by assigning transfer coefficients between compartments reflecting physicochemical drug properties.¹

The PBPK approach can be more powerfully applied using computational fluid dynamics (CFD), which uses numerical methods to provide approximate solutions to the differential equations that describe fluid flow, heat transfer, and species transport. Today's CFD software tools are general enough such that the same software used to model product performance in such diverse fields as automotive, nautical, aeronautical, civil, and petroleum engineering can be applied to predict the flow of fluid, heat and drug in the eye. A primary advantage over compartmental approaches is that CFD models the spatial distribution of drug within each compartment through time. Such detailed numerical experimentation can help establish the safety and efficacy of a delivery system while reducing the number and/or size of clinical studies required.

OCULAR CFD MODEL SUMMARY

This section provides an introduction to the physical processes that govern fluid flow, heat transfer, and drug motion in the eye and their implementation into a CFD model, please see Missel *et al*, 2010 for a complete description.²

A CFD simulation begins with the construction of a geometric model that includes all structures involved in fluid, heat, and drug transport. The geometry is typically constructed in CAD or a geometry tool specific to the CFD software. Figure 1 shows anatomical human and rabbit ocular models. The rabbit is frequently used as a preclinical model for evaluating ophthalmic drug products before human clinical testing. Conducting simulations in both ocular



Dr Paul Missel
Therapeutic Area Modeller
Modelling & Simulation
Global Clinical and Regulatory Affairs
T: +1 817 551 4926
E: paul.missel@alcon.com

Alcon Research, Ltd
TC-47, 6201 South Freeway
Fort Worth, TX 76134
United States

www.alcon.com



Dr Marc Horner
Lead Technical Services Engineer,
Healthcare
T: +1 847 491 0200
F: +1 847 869 6495
E: marc.horner@ansys.com

ANSYS, Inc
2600 Ansys Drive
Canonsburg, PA 15317
United States

www.ansys.com

geometries enables translating results from preclinical experiments in rabbits into predictions for clinical outcomes in humans.

The aqueous humour region consists of the fluid zones between the cornea and vitreous, excluding the iris and ciliary body. Aqueous humour is a clear, non-viscous, water-like fluid that is secreted by cells on the outer lining of the ciliary body. Aqueous humour flows around the iris and exits the eye through the trabecular meshwork, a ring-shaped structure of connective tissue. Aqueous humour following this path eventually returns to the blood via a fine venous network surrounding the outer layer of the sclera, the shell encasing most of the eye. A small fraction of aqueous humour percolates through the sclera and cornea. The resistance of the sclera to fluid permeation produces the intra-ocular pressure. The trabecular meshwork also provides some resistance to fluid flow and in glaucoma this resistance increases, thus increasing the pressure.

All structures apart from aqueous humour were treated as porous media. Experimental measurements have established the hydraulic resistance of the sclera is about 15,000 times higher than that of the vitreous. All other porous media tissues, apart from the trabecular meshwork and the vitreous, are assigned the same resistance as the sclera. The hydraulic resistance of the trabecular meshwork was a parameter in the model whose value was adjusted such that the maximum pressure inside the eye matched an intraocular pressure of 15 Torr. A band along the ciliary body behind the iris produces aqueous humour at a rate appropriate for each species. The pressure

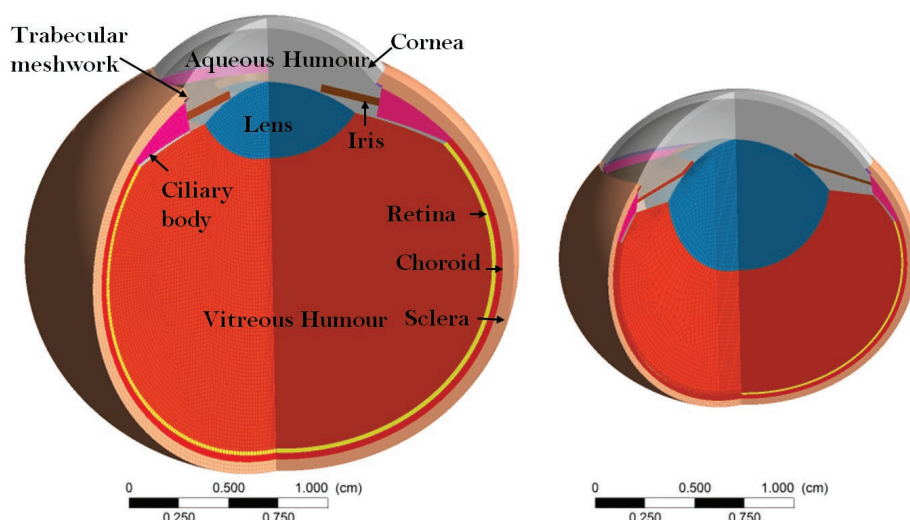


Figure 1: Comparison of geometric ocular models for human and rabbit, shown on the same scale; the horizontal bar below each panel corresponds to 1 cm.⁸

boundary condition on the outer sclera and the surface behind the trabecular meshwork was specified as 10 Torr, matching the episcleral venous pressure, whereas there was zero (atmospheric) pressure applied on the outer cornea. The sclera, choroid, retina, iris and ciliary body were set to a fixed temperature of 37°C and the cornea was set to 34°C. The thermal gradient between the cornea and internal tissues creates density gradients in the aqueous humour, which significantly impact aqueous flow patterns.

The fluidic and thermal transport processes were simulated using the ANSYS Fluent CFD solver. Figure 2 shows simulation results of pressure, temperature and fluid flow in the rabbit ocular model. In Figure 2a, most of the ocular interior is at the maximum pressure of 15 Torr; the pressure drop occurs almost entirely across

the outer sheath surfaces. Figure 2b shows the variation of temperature within the eye. Since the aqueous humour density is allowed to vary with temperature, density gradients give rise to thermal convection, which creates a circulating flow pattern with a maximum fluid velocity on the order of 10^{-4} m/s, as illustrated in Figure 2c. The maximum velocity for the hydraulic flow in the vitreous is four orders of magnitude lower than the maximum velocity within the aqueous humour region. This fluid-thermal solution forms the baseline convective flow pattern upon which the modes of drug delivery presented in the next three sections occur.

MODEL APPLICATION: PK FOLLOWING TOPICAL DELIVERY

Topical dosing is commonly used to treat glaucoma. The target of anti-glaucoma drugs is typically the iris / ciliary body. Mechanisms of action include reducing the production rate for aqueous humour and reducing the hydraulic resistance of the iris root to facilitate outflow. Topically administered anti-inflammatory drugs also target the iris / ciliary body to reduce pain and inflammation following cataract surgery. These drugs can also exert an important influence on deeper ocular tissues such as the retina and macula to prevent edema, which occurs occasionally in diabetic patients following surgery.

Drug transport in the eye was also simulated using ANSYS Fluent, which can model the interaction between drug convection, diffusion and elimination. Convection is the motion of drug due to bulk flow of aqueous humour; diffusion is the rate of passive mass transport through the medium down

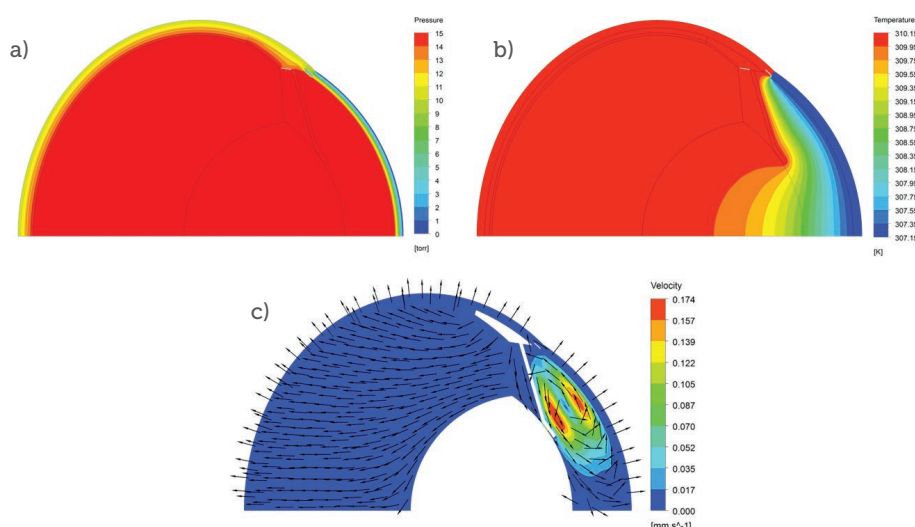


Figure 2: CFD simulation results in the rabbit eye model. a) Pressure (Torr). b) Temperature (Kelvin). c) Vector velocity, arrows show direction of flow and are colour-coded to match the scale for the superimposed contour plot (m/s).

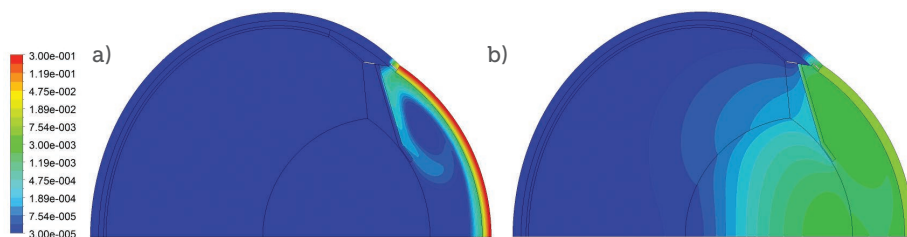


Figure 3: Simulated advection of drug into ocular tissue following topical dosing with timolol maleate (concentration plotted on a logarithmic scale where 1 corresponds to the concentration of drug in the topical dose). a) Three minutes after instillation of a topical dose. b) Four hours after instillation.

a concentration gradient, and sink terms account for removal of drug by vascular or lymphatic clearance. Chemical partitioning, which gives rise to discontinuities in drug concentration at boundaries between tissues having different lipophilic / hydrophilic properties, is also included in the model through the use of jump conditions at tissue interfaces. Each tissue is assigned its own unique set of values for the partition coefficient, diffusion coefficient, sink term, and equilibrium drug concentration.

Drug application to the outer corneal surface can be modelled by a time-varying function approximating the tear concentration resulting from instillation of a topical dose. The tear film concentration decays exponentially with time, the concentration dynamics being influenced by the initial rapid decrease in pre-corneal fluid volume after dosing and by the continuous influx of fresh tears. Since our models do not include tissues outside the eye such as the conjunctiva and eyelids, our drug input function will most likely overestimate the flux of drug into the eye. Thus we include a single

adjustable parameter to enable tuning the amplitude of the drug input function. The model predicts that rapid mixing of aqueous humour in the anterior chamber creates a wisp of higher drug concentration just a few minutes after drug instillation (Figure 3a). Mixing has rendered the aqueous humour drug concentration to be approximately uniform four hours later (Figure 3b).

Figure 4 compares simulation results with experimental measurements of mean tissue concentrations following the topical dosing of a drug solution. The concentrations in the anterior compartments initially increase with time, then decrease as drug distributes throughout the remaining tissues. Applying an amplitude prefactor of one quarter for our drug input function, the simulation accurately predicts the time dependence of the concentrations for anterior tissues such as the iris / ciliary body, the tissue affected by the drug. Thus, CFD is quite useful for predicting the time course of drug distribution. Simulated concentrations in the vitreous and lens lag behind the experimental values, however. Additional fluid currents

or vascular circulation pathways capable of transporting drug between tissue compartments may be at work. Identifying and incorporating these missing fluidic and circulatory currents could improve the model.

MODEL APPLICATION: DELIVERY FROM INTRAOCCULAR DEPOTS

Much effort has been expended in development of bio-erodible dosage forms that will sustain drug release over time. However, a suspension may perform suitably as a sustained release depot if injected in a region of quiescent vitreous which has retained its gel-like consistency, provided that the drug solubility is low enough to dissolve slowly but high enough to deliver a therapeutic level of drug. Drug release rate and duration can be controlled by adjusting the suspension drug concentration. This behaviour is a consequence of a local concentration effect, in which drug dissolved from one particle suppresses the dissolution of drug from nearby particles. The formulation will need to be engineered to immobilise the particles until they are completely dissolved for this approach to be most effective.

Figures 5 and 6 show simulation results from various model suspensions of triamcinolone acetonide (TAC). In each simulation, identically sized particles are initially arranged in an evenly spaced array inside a spherically shaped depot.

Figure 5 illustrates how the duration of the suspension (defined as the time after injection at which all solid drug has dissolved) varies with particle size. Figure 6 shows the time dependence of drug content for two different suspensions. These simulations utilised the volume of fluid (VOF) method in ANSYS Fluent, which enables the tracking of phase boundaries through a stationary mesh. In this case, the VOF method tracks the boundary between solid, undissolved drug crystals and drug dissolved in solution. The concentration at the dissolving surface was set to 36 ppm, the drug solubility limit.

The insets in Figure 5 show the quasi steady-state drug distributions a few days after intravitreal injection. The contours show the drug concentration in the region containing the particles is very close to the solubility limit (denoted by the red colour). The concentration decreases at a rate that is approximately inversely proportional to distance outside the suspension depot. If the therapeutic window (the difference between the minimum effective

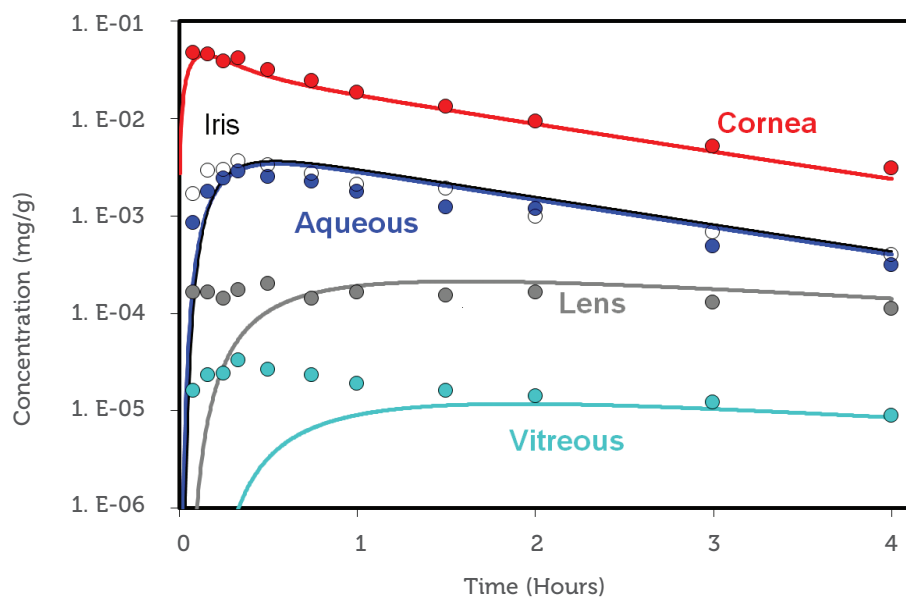


Figure 4: Comparison of simulated & experimental mean tissue compartment concentrations following topical instillation of 25 μ L 0.65% timolol maleate.⁹

concentration and the maximum concentration allowable before toxic side effects are manifested) is wide enough, the entire eye may be treated effectively.

For an oral suspension dissolving in the stomach, drug particles dissolve at a rate proportional to the total particle surface area, as specified by the Noyes-Whitney equation.³ This strong dependence of dissolution rate on particle surface area is observed in certain *in vitro* dissolution experiments which expose drug particles to copious amounts of dissolution medium under substantial agitation.⁴ Each particle is uniformly accessible to the release medium in these methods. This is not the case for the intravitreal depot, because the particles on the exterior shield interior particles from dissolution. Instead, the dependence of dissolution rate on particle size exhibits an asymptote. The arrow in Figure 5 at 428 μ m identifies the diameter at which the dissolution rate is within 1% of the value in the limit of infinitesimally small particle size. Since this diameter is 30-100 times the diameter of particles in a typical ophthalmic suspension, dissolution rate of an intravitreal depot will not depend on particle size.

Figure 6 shows a comparison between simulated dissolution-*versus*-time profiles for suspensions containing either 4 or 16 mg TAC confined to a 100 μ L spherical depot versus simulations in the infinitesimally small particle size limit. The predictions match the experimental data fairly well for the 16 mg depots, but under-predict the duration of the 4 mg depots. If we allow for the depot to condense to a smaller volume after day 10, as was observed in the 2006 study by Kim *et al.*,⁵ the simulation curve for 4 mg comes in closer agreement with the data.

MODEL APPLICATION: JUXTASCLERAL DEVICES

Our last example is a juxtasclear device for anecortave acetate (AAc), a low-molecular-weight lipophilic compound which at one time was being developed to treat macular degeneration. The prototype device, shown in Figure 7a, is a silicone holder for placing a drug tablet adjacent to the sclera. A simulation for steady-state drug distribution in ocular tissue is shown in Figure 7b. Drug partition and diffusion coefficients were obtained from *in vitro* experiments equilibrating ocular tissues with drug solution and measuring drug permeability through excised tissues.⁶ Partition coefficients for drug are 2.2 and 4 for sclera and

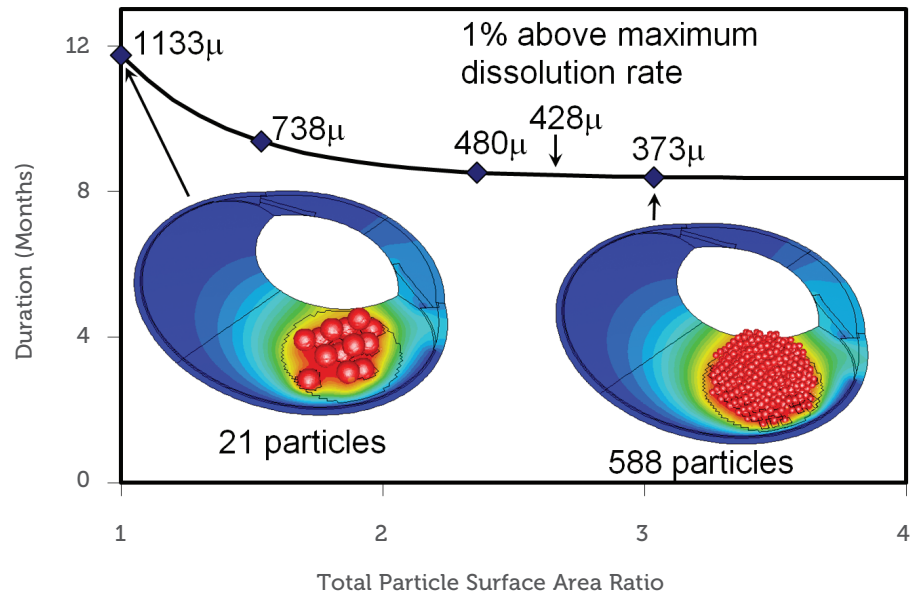


Figure 5: Influence of particle size on duration of suspensions of 16 mg TAC confined to a 100 μ L spherical vitreous depot. The units of the horizontal axis denote the ratio in total particle surface area compared to the model suspension with the largest particle size simulated. The insets show model suspensions dividing the drug into either 21 (left) or 588 (right) equally sized spherical particles. The colour spectrum denotes drug concentration, red corresponding to the solubility limit and blue corresponding to zero drug concentration. Duration becomes quite insensitive to particle size when the size falls below 428 μ m in diameter. This simulation used an earlier rendition of the rabbit eye geometry in which the lens was represented by an appropriately shaped void.²

retina/choroid respectively; this partitioning is apparent in the figure contours. The strength of the choroidal drug sink was adjusted to match drug clearance rate after

intravitreal injection of a dilute AAc solution. This sink localises delivery to a region immediately beneath the tablet.

Juxtasclear devices containing AAc

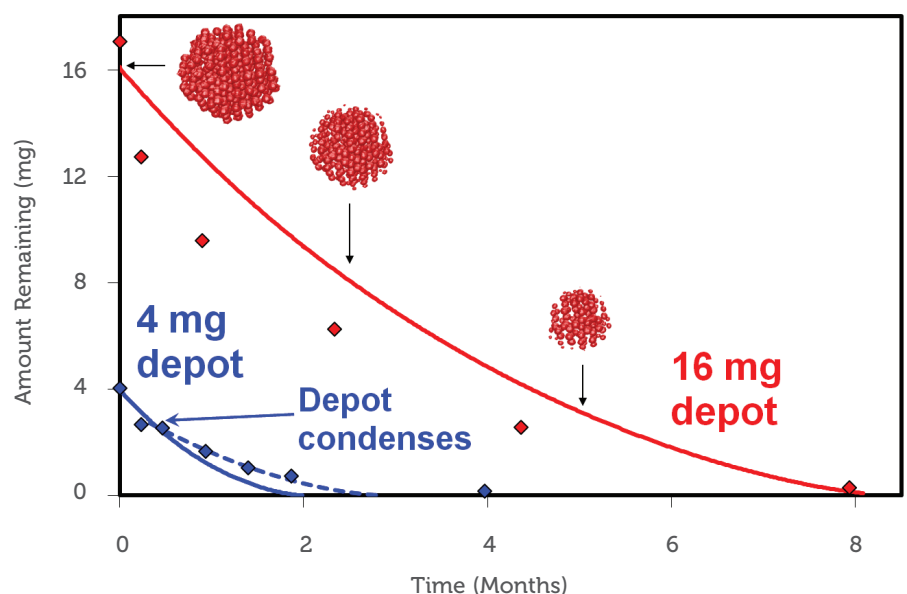


Figure 6: Dissolution versus time profiles for 4 mg and 16 mg TAC confined to a 100 μ L spherical vitreous depot compared with experimental data from Kim 2006 (diamonds).⁵ Curves represent simulation predictions in the limit of infinitesimally small particles. The appearance of the 276-particle suspension model at various times is shown in the insets. The dashed curve for 4 mg restarts the simulation by distributing 2.7 mg of drug in a 25 μ L depot on day 10 to approximate the influence of depot condensation observed *in vivo*.²

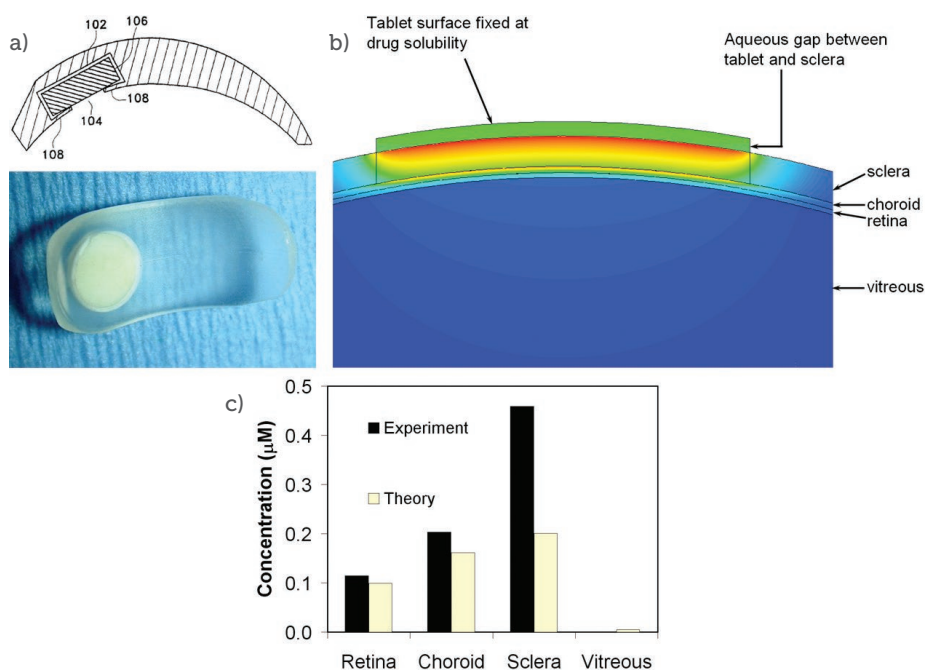


Figure 7: a) Upper panel: Schematic for juxtасlеral device 10: 102 – cavity; 106 – drug source; 104 – exposed opening; 108 – circumferential rim to retain the drug source. Lower panel: photo of prototype device. b) Simulated steady-state drug concentration in ocular tissue resulting from delivery of AAC from the device. c) Comparison between experimental and simulated average concentrations in the measured tissues at the one year following implantation of juxtасlеral devices containing AAC in rabbits.^{7,11}

implanted in rabbits maintained constant ocular tissue drug levels for two years. Figure 7c shows average drug levels in retina, choroid and sclera in a 10 mm circular dissection beneath the depot one year after insertion. Since the device provides for unidirectional release of drug towards the ocular interior, and shields from non-productive loss behind the eye, the payload duration is extended. The simulated tissue concentration is ranked Sclera > Choroid > Retina >> Vitreous. Using no additional adjustable parameters, simulations predict the appropriate rank order and come close to the values measured in the retina and choroid. The values for sclera match less well, but less is known about the exterior scleral sinks.

CONCLUSION

The examples described in this article illustrate some of the capabilities of computational fluid dynamics to model ocular drug delivery. Its application is limited, however, by the accuracy and completeness of the ocular anatomy and by the particular features of ocular physiology incorporated into the model. For example, the lack of external anterior ocular anatomical features limits the ability to apply the current model to topical delivery.

The number of publications utilising methods similar to what is described here are increasing. Many additional aspects have been explored, such as the effects of age and disease on liquefaction of the vitreous, eye movements, and variability in permeability of the outer tissue layers. Simulations may also provide insights into the effect of various disease states on drug delivery. Such work needs to be guided and qualified by appropriate preclinical and clinical observations to maximise the insights provided.

The design of ophthalmic drug delivery therapies can be improved as the fluidic and vascular clearance barriers are better understood through careful *in vivo* experiments illuminated through simulation.

ACKNOWLEDGEMENT

The authors would like to thank Lasya Reddy of ANSYS, Inc, for her assistance creating some of the images for this article.

REFERENCES

1. Zhang W, Prausnitz MR, Edwards A, "Model of transient drug diffusion across the cornea". *J Controlled Release*, 2004, Vol 99, pp 241-258.
2. Missel PJ, Horner M, Muralikrishnan

R, "Dissolution of intravitreal triamcinolone acetonide suspensions in an anatomically accurate rabbit eye model". *Pharm Res*, 2010, Vol 27, pp 1530-1546.

3. Noyes AA, Whitney WR. *J Am Chem Soc*, 1897, Vol 19, pp 930-934.
4. Mauger JW, Howard SA, Amin K, "Dissolution profiles for finely divided drug suspensions. *J Pharm Sci*, 1983, Vol 72, pp 190-193.
5. Kim H, Csaky KG, Gravlin L, Yuan P, Lutz R, Bungay P, Tansey G, De Monasterio F, Potti GK, Grimes G, Robinson RM, "Safety and pharmacokinetics of a preservative-free triamcinolone acetonide formulation for intravitreal administration". *Retina*, 2006, Vol 26, pp 523-530.
6. Missel P, Chastain J, Mitra A, Kompella U, Kansara V, Duwvuri S, Amrite A, Cheruvu N, "In vitro transport and partitioning of AL-4940, active metabolite of angiostatic agent anecortave acetate, in ocular tissues of the posterior segment". *J Ocular Pharmacol Ther*, 2010, Vol 26, pp 137 – 145.
7. Missel P, "Computer Modeling of Pharmacokinetics from Ocular Drug Delivery". Lecture presented at the 2009 Association for Research in Vision and Ophthalmology Summer Eye Research Conference on Ophthalmic Drug Delivery Systems for the Treatment of Retinal Diseases: Basic Research to Clinical Application, Bethesda, MD, US.
8. Missel P, "Simulating intravitreal injections in anatomically accurate models for rabbit, monkey and human eyes". *Pharm Res*, 2012, Vol 29, pp 3251-3272.
9. Francoeur ML, Sitek SJ, Costello B, Patton TF, "Kinetic disposition and distribution of timolol in the rabbit eye. A physiologically based ocular model". *Int J Pharm*, 1985, Vol 25, pp 275-292.
10. Missel P, Yaacobi Y, "Drug Delivery Device". 2011, US Patent 7,943,162.
11. Missel P, "Computer modeling for ocular drug delivery. In *Ocular Drug Delivery Systems: Barriers and Application of Nanoparticulate Systems*", Thassu D, Chader GJ eds., CRC Press, 2013 Boca Raton, FL, US.